



ORIGINAL ARTICLE

The spatial distribution of immune cell subpopulations in hepatocellular carcinoma

Peng-Cheng Wang^{1,2}  | Zhi-Qiang Hu^{1,3} | Shao-Lai Zhou^{1,3}  | Song-Yang Yu^{1,3} | Li Mao^{1,3} | Sheng Su^{1,3} | Jia Li^{1,3} | Ning Ren^{1,2,3} | Xiao-Wu Huang^{1,3}

¹Key Laboratory of Carcinogenesis and Cancer Invasion (Fudan University), Ministry of Education, Shanghai, China

²Key Laboratory of Whole-period Monitoring and Precise Intervention of Digestive Cancer (SMHC), Minhang Hospital & AHS, Fudan University, Shanghai, China

³Department of Liver Surgery and Transplantation, Liver Cancer Institute, Zhongshan Hospital, Fudan University, Shanghai, China

Correspondence

Xiao-Wu Huang and Ning Ren, Department of Liver Surgery and Transplantation, Liver Cancer Institute, Zhongshan Hospital, Fudan University, 180 Fenglin Road, Shanghai 200032, China.

Emails: huang.xiaowu@zs-hospital.sh.cn; ren.ning@zs-hospital.sh.cn

Funding information

National Natural Science Foundation of China, Grant/Award Number: 81472672 and 91942313; Major Special Projects of the Ministry of Science and Technology, Grant/Award Number: 2018ZX10302207; Shanghai International Science and Technology Collaboration Program, Grant/Award Number: 18410721900; Fundamental Medical Project of Minhang Hospital of the Fudan University Project Foundation, Grant/Award Number: 2020MHJC06

Abstract

Infiltrating immune cells in the tumor microenvironment (TME) influence tumor progression and patient prognosis, making them attractive therapeutic targets for immunotherapy research. A deeper understanding of immune cell distributions in the TME in hepatocellular carcinoma (HCC) is needed to identify interactions among different immune cell types that might impact the effectiveness of potential immunotherapies. We performed multiplex immunohistochemistry using a tissue microarray of samples from 302 patients with HCC to elucidate the spatial distributions of immune cell subpopulations (CD3⁺, CD4⁺, CD8⁺, CD66b⁺, and CD68⁺) in HCC and normal liver tissues. We analyzed the associations between different immune subpopulations using Pearson's correlation. G(r) functions, K(r) functions and Euclidean distance were applied to characterize the bivariate distribution patterns among the immune cell types. Cox regression and Kaplan-Meier analysis were used to evaluate the associations between tumor infiltration by different immune cells and patient outcomes after curative surgery. We also analyzed the relationship between the spatial distribution of different immune cell subpopulations with HCC patient prognosis. We found that the immune cell spatial distribution in the HCC TME is heterogeneous. Our study provides a theoretical basis for HCC immunotherapy.

KEYWORDS

hepatocellular carcinoma, immune cell subpopulations, multiplex immunohistochemistry, prognosis, tumor microenvironment

Abbreviations: HCC, Hepatocellular carcinoma; IHC, Immunohistochemistry; OS, Overall survival; TME, Tumor microenvironment.

Peng-Cheng Wang and Zhi-Qiang Hu authors contributed equally to this paper.

This is an open access article under the terms of the Creative Commons Attribution-NonCommercial-NoDerivs License, which permits use and distribution in any medium, provided the original work is properly cited, the use is non-commercial and no modifications or adaptations are made.

© 2021 The Authors. *Cancer Science* published by John Wiley & Sons Australia, Ltd on behalf of Japanese Cancer Association.

1 | INTRODUCTION

Hepatocellular carcinoma (HCC) has high recurrence and mortality rates, making it one of the most lethal forms of cancer.¹ In early 1990s, cytokine immunotherapy was proposed as a new treatment modality for HCC.² Immunotherapy with anti-programmed cell death protein 1 (PD-1) agents has achieved encouraging results against various tumor types, including breast cancer³ and non-small-cell lung cancer.⁴ However, the response rate to immunotherapy in patients with HCC remains unsatisfactory, primarily due to a lack of understanding of the spatial context of the highly heterogeneous tumor microenvironment (TME).⁵

The TME is a cellular environment comprising stromal cells, the extracellular matrix, immune cells, and malignant cells.⁶ Tumors depend on the TME for growth because interactions among cellular compartments are vital for both tumor cells and stromal cells.⁷ CD8⁺ T cells, CD4⁺ T helper 1 (Th1) cells, and the secreted cytokine interferon gamma suppress tumor development,⁸ whereas tumor-associated neutrophils recruit macrophages and regulatory T cells to promote tumor growth and resistance to the anti-cancer drug sorafenib.⁹ In addition, the PD-1/programmed cell death-ligand 1 (PD-L1) axis interacts with certain mutations in tumor cells to modulate antitumor immunity because upregulation of PD-L1 inhibits T cell effector functions.¹⁰ Importantly, few studies have investigated the spatial relationships among different types of immune cells within the TME.

Multiplex immunohistochemistry (IHC) provides more information than traditional IHC and has emerged as a crucial tool in TME studies.¹¹ We used multispectral quantitative fluorescent IHC to explore the spatial distributions of immune cells in the TME and found that the distribution of immune cells was heterogeneous between HCC tumor tissues and normal tissues. We also found that the immune cell distribution was associated with patient prognosis.

2 | MATERIALS AND METHODS

2.1 | Patient information and specimens

We performed multiplex IHC using a tissue microarray of matched tumor and non-tumor liver samples from the 302 patients with HCC who had undergone curative resection at the Liver Cancer Institute, Zhongshan hospital, Fudan University between January 2003 and March 2004. Patients with distant metastasis or any history of treatment for HCC were excluded from the study. All patients were diagnosed with HCC based on postoperative pathology evaluation. The Zhongshan Hospital Research Ethics Committee granted ethical approval for the study of human subjects. The American Joint Committee on Cancer staging system was used to determine the tumor grade in each patient.¹²

2.2 | Tissue microarrays and multiplexed immunohistochemistry

We constructed tissue microarrays as previously described¹³ using 2 tumor and 2 non-tumor core specimens from each patient, each with a diameter of 1.5 mm. For multiplex IHC analysis of the microarrays, we used the Opal 7-Color Fluorescent IHC Kit in accordance with the manufacturer's protocol (NEL811001KT; PerkinElmer) with the following fluorescent markers: DAPI (1:100; ab104139; abcam), anti-CD3 (1:100; ab16669; abcam), anti-CD4 (1:500; ab133616; abcam), anti-CD8 (1:200; #85336; CST), anti-CD66b (1:100; ab197678; abcam), and anti-CD68 (1:100; ab783; abcam). Opal multiplexing is a serial IHC method that relies on tyramide single amplification. Opal slides can be visualized using standard fluorescence microscopy. Multispectral imaging allows quantitative unmixing of various fluorophores and removal of tissue autofluorescence. We analyzed fluorescence microscopy images using Inform image analysis software (version 2.4; PerkinElmer). All representative images were chosen by 3 pathologists.

2.3 | Quantification of the spatial distribution of immune cells

We used a bivariate point pattern characterized by the bivariate $G(r)$ and $K(r)$ functions to represent the relative spatial distributions of immune cell subpopulations.¹⁴ The bivariate $G(r)$ function is defined as a probability function of the nearest neighbor distance within a given radius and the formula is:

$$G(r) = \frac{\sum [i,j] I(d[i,j] \leq r)}{n}$$

The bivariate $K(r)$ function is defined as the expected number of cells appearing within the radius and the formula is:

$$K(r) = (\alpha / (n^* (n-1))) * \sum [i,j] I(d[i,j] \leq r) e[i,j]$$

In both functions, the distance between 2 points is defined as $d[i,j]$, the logical decision function within the radius is defined as $I(d[i,j] \leq r)$, α is the acreage, n is the count of cells, and r is the radius of the area in which the function is evaluated. As a null hypothesis, we assume that the different types of immune cells are independent of each other, and that the distances between nearest neighbors from different cell types follow a Poisson distribution.

The Euclidean distance between 2 points $u = (u_1, u_2)$ and $v = (v_1, v_2)$ is defined as follows:

$$\|u - v\| = \left[(u_1 - v_1)^2 + (u_2 - v_2)^2 \right]^{1/2}$$

We calculated the G(r), K(r) functions, and the distance between 2 different immune cell subpopulations using the toolbox 'spatstat' in R.

2.4 | Statistical analysis

We used SPSS, version 23.0 (IBM Corporation) for all statistical analyses. We performed two-way comparisons between groups using the Student's t-test and analyzed differences in OS using the Kaplan-Meier method and log-rank test. We used univariate and multivariate Cox proportional hazard models to calculate associations between the survival outcomes and clinicopathologic characteristics. We applied Pearson's correlation coefficient (*R*) to evaluate potential correlations between the groups. We used $*P < .05$ as the threshold for significance in all statistical tests.

3 | RESULTS

3.1 | Patient and disease characteristics

Our study sample included 302 patients with primary HCC who had undergone curative resection. Most of the patients were male ($n = 257, 85.1\%$) and had a history of hepatitis B virus (HBV) infection ($n = 264, 87.4\%$). The median age was 50 y, and the median tumor diameter was 5.0 cm. In accordance with the American Joint Committee on Cancer staging system, 51.0% ($n = 154$) of the patients had T1 disease. Post-surgical histologic evaluation of the tumor tissues by 3 independent pathologists determined that most tumors were moderately differentiated ($n = 239, 79.1\%$), and almost half ($n = 138, 45.7\%$) had vascular invasion (Table 1).

3.2 | Heterogeneous immune cell subpopulations infiltrated the HCC tumors

We characterized immune cell distribution in the HCC tumors using multiplex IHC, which allowed simultaneous visualization of 5 markers in each formalin-fixed and paraffin-embedded tissue section. To explore the subpopulations of immune cells in HCC, we used fluorescent antibodies to visualize CD3, CD4, CD8, CD66b, and CD68. We also used DAPI as a nuclear stain. In addition to the shape of nucleus, the marker CD3 was used to identify all T cells. We defined CD3⁺CD8⁺CD4⁻ cells as cytotoxic T cells, CD3⁺CD8⁻CD4⁺ cells as CD4⁺ T cells, and any other cells with CD3⁺ staining that were negative for the other 2 markers as "other T cells" (CD3⁺CD8⁻CD4⁻). We defined CD68⁺ cells as macrophages and CD66b⁺ cells as neutrophils. To minimize false-positive results, we applied co-localization in our process to identify the different immune cell populations. Representative images of the different cells in tumor tissue and non-tumor tissues are shown in Figure 1 and Figure S1, respectively.

TABLE 1 Patient clinical information (n = 302)

Clinicopathologic index		
Age (y)	≤50	157 (52.0%)
	>50	145 (48.0%)
Sex	Female	45 (14.9%)
	Male	257 (85.1%)
HBsAg	Negative	38 (12.6%)
	Positive	264 (87.4%)
HCV	Negative	295 (97.7%)
	Positive	7 (2.3%)
AFP (ng/ml)	≤20	90 (29.7%)
	>20	212 (70.3%)
GGT (U/L)	≤54	124 (41.1%)
	>54	178 (58.9%)
Liver cirrhosis	No	33 (10.9%)
	Yes	269 (89.1%)
Tumor size (cm)	≤5	143 (47.4%)
	>5	159 (52.6%)
Tumor number	Single	255 (84.4%)
	Multiple	47 (15.6%)
Microvascular invasion	Absence	164 (54.3%)
	Present	138 (45.7%)
Tumor encapsulation	Complete	149 (49.3%)
	None	153 (50.7%)
Tumor differentiation	I+II	239 (79.1%)
	III+IV	63 (20.9%)
TNM stage	I	154 (51.0%)
	II+III	148 (49.0%)

Note: AFP, alpha-fetoprotein; GGT, gamma glutamyl transferase; TNM, tumor-node-metastasis.

When we compared the immune cell distributions between tumor and non-tumor tissues, lower proportions of CD3⁺ T cells were observed in the tumor tissues (6.45% vs. 2.69%; $*P < .001$; Figure 2A). Furthermore, the proportion of CD3⁺ T cells that were CD4⁺ was lower in the non-tumor tissues than in matched tumor tissues (9.53% vs. 16.12%; $*P < .05$; Figure 2B). Conversely, the proportion of CD3⁺ T cells that were CD8⁺ was higher in tumor tissues than in non-tumor tissues (34.58% vs. 30.55%; $*P < .001$; Figure 2C).

3.3 | Different immune cell subpopulations aggregated together in HCC tumors

Tumor tissues contain various immune cells that interact to maintain the physiological function of the TME. The presence of neutrophils was correlated with that of CD8⁺ T cells in HCC tumor tissues ($R = 0.145$; $*P < .05$; Figure 3A), and the presence of neutrophils in tumor tissues was correlated with that of macrophages

($R = 0.440$; $**P < .001$; Figure 3A). Strikingly, the presence of neutrophils in tumor tissues was also correlated with that of $CD4^+$ T cells ($R = 0.183$; $**P < .001$; Figure 3A).

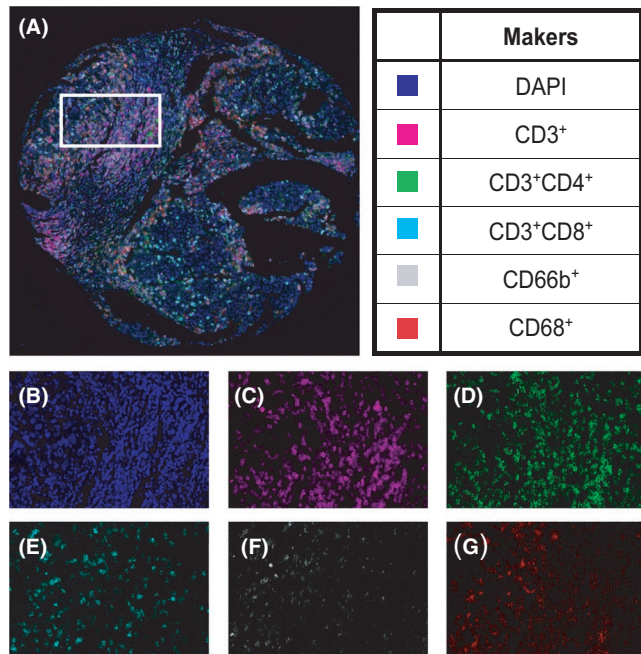


FIGURE 1 Multiplex immunohistochemistry of primary HCC identifies unique immune cell subtypes. A, Representative multispectral image of HCC tumor sample on tissue microarray. B-G, The presence of individual markers before spectral mixing: (B) DAPI nuclear marker, (C) CD3, (D) CD4, (E) CD8, (F) CD66b, (G) CD68

Carstens and colleagues used K-functions and L-functions (the deformed variants of K-functions) to characterize the spatial patterns of pancreatic cancer cells and intratumoral T cells.¹⁴ We combined $G(r)$ and $K(r)$ functions to make our results more reliable (Figure 3B-E). The blue line represents the theoretical distribution of distances between cells in 2 different immune subpopulations, which we assume conforms to a Poisson distribution. The red line represents the actual distribution of those distances. Values of r ranging from 0 to 30 μm are considered ideal to calculate the spatial relationship between 2 cell populations.¹⁵ When the red line is above the blue line, the aggregation patterns of 2 the cell types under consideration cannot be considered independent. Conversely, if the red line was below the blue line, the aggregation patterns of the 2 cell types can be considered independent. In the plot of the $G(r)$ and $K(r)$ functions for macrophages and neutrophils, the red line is above the blue line, indicating that macrophages and neutrophils tended to aggregate closer together than would be expected if their spatial distributions were independent (Figure 3C). The aggregation patterns of $CD8^+$ T cells with neutrophils and $CD4^+$ T cells with neutrophils were not independent of each other in HCC (Figure 3D,E). The spatial distributions of different immune cell populations in non-tumor tissues are shown in Figure S2.

3.4 | Immune cell infiltration correlated with HCC prognosis

We used patient follow-up information to further explore the correlation between infiltrating immune cells and patient outcomes

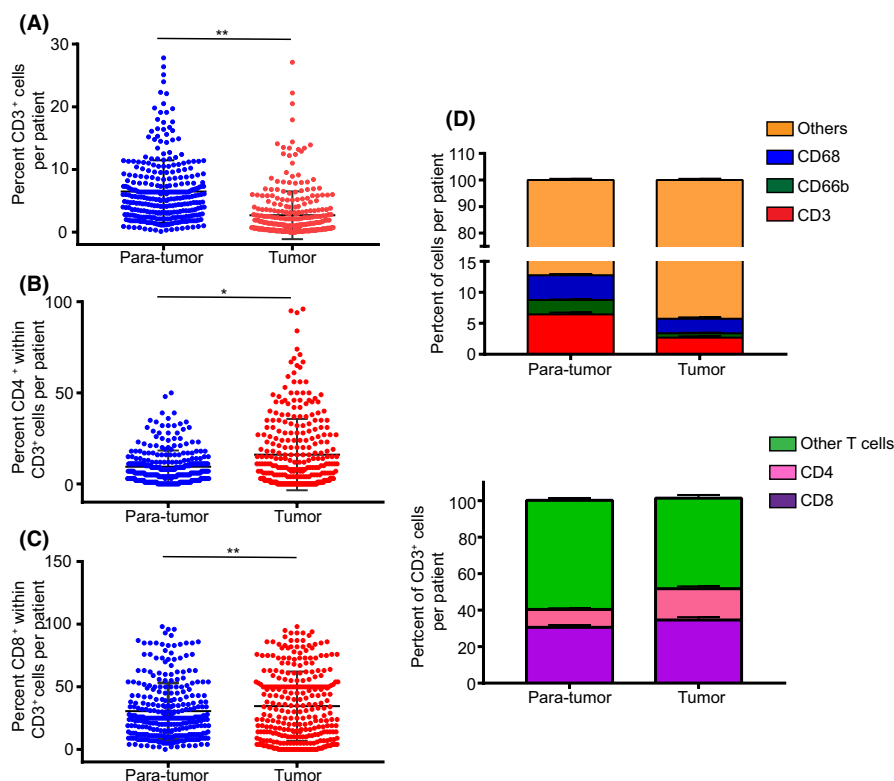


FIGURE 2 Heterogeneous immune cell subpopulations infiltrating in HCC tissues. A, $CD3^+$ T cells were more abundant in normal tissues than in tumors ($**P < .001$). B, Percentage of $CD4^+$ T cells within the $CD3^+$ T cell population was lower in normal tissues than in tumors ($*P < .05$). C, Percentage of $CD8^+$ T cells within the $CD3^+$ T cell population was lower in normal tissues than in tumors ($**P < .001$). D, Distribution of different immune cell subpopulations within defined groups is shown

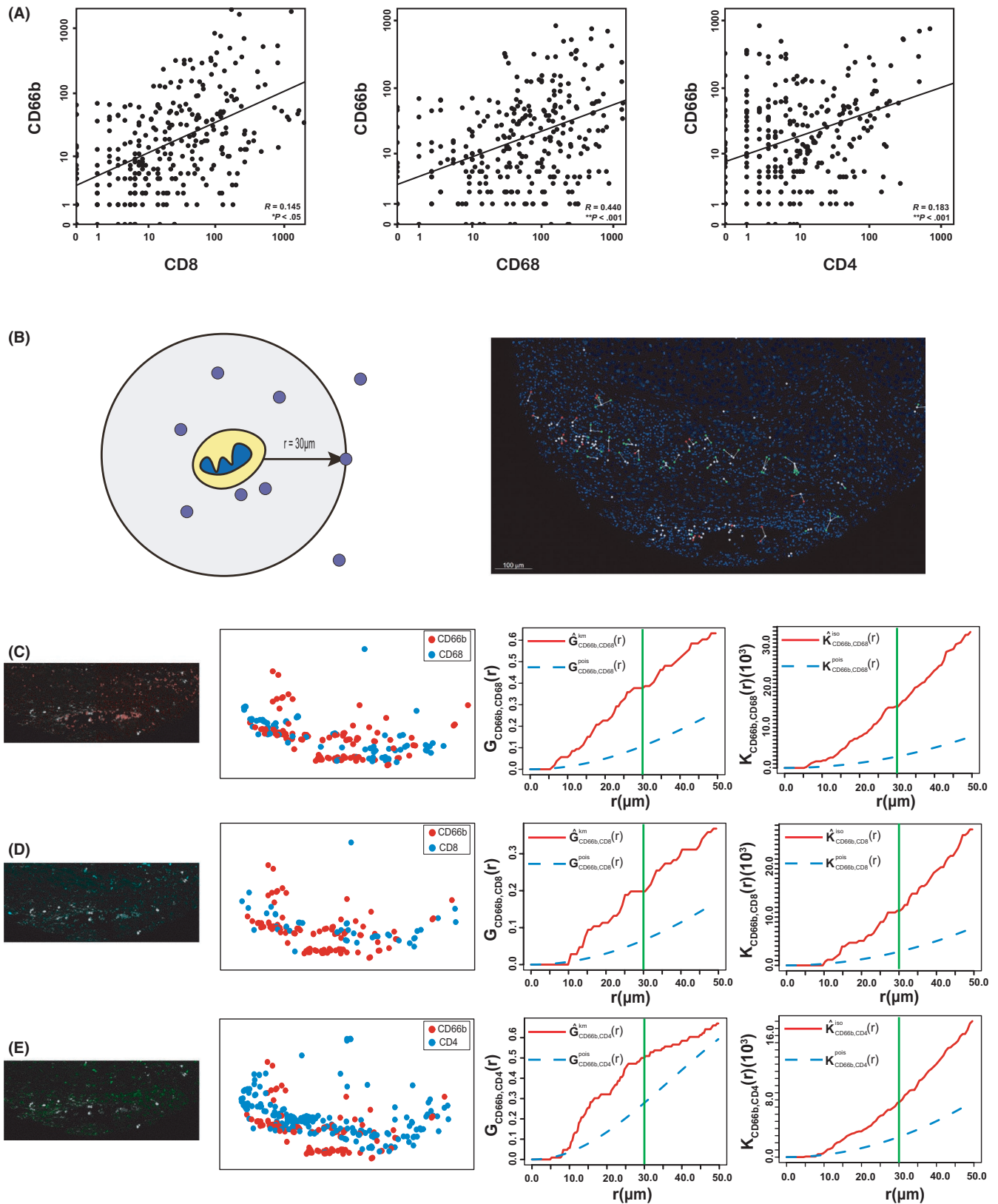


FIGURE 3 Associations between different immune cell types. A, Intratumoral spatial distribution of CD66b⁺ cells (neutrophils) was positively correlated with those of CD8⁺ T cells ($R = 0.145$, $*P < .05$), CD68⁺ cells (macrophages) ($R = 0.440$, $**P < .001$), and CD4⁺ T cells ($R = 0.183$, $**P < .001$). B, Cell phenotype map showing the spatial distributions of different immune cell populations. C–E, $G(r)$ and $K(r)$ functions were used to characterize the observed and expected aggregation patterns between (C) CD66b⁺ cells and CD68⁺ cells, (D) CD66b⁺ cells and CD8⁺ cells, and (E) CD66b⁺ cells and CD4⁺ cells

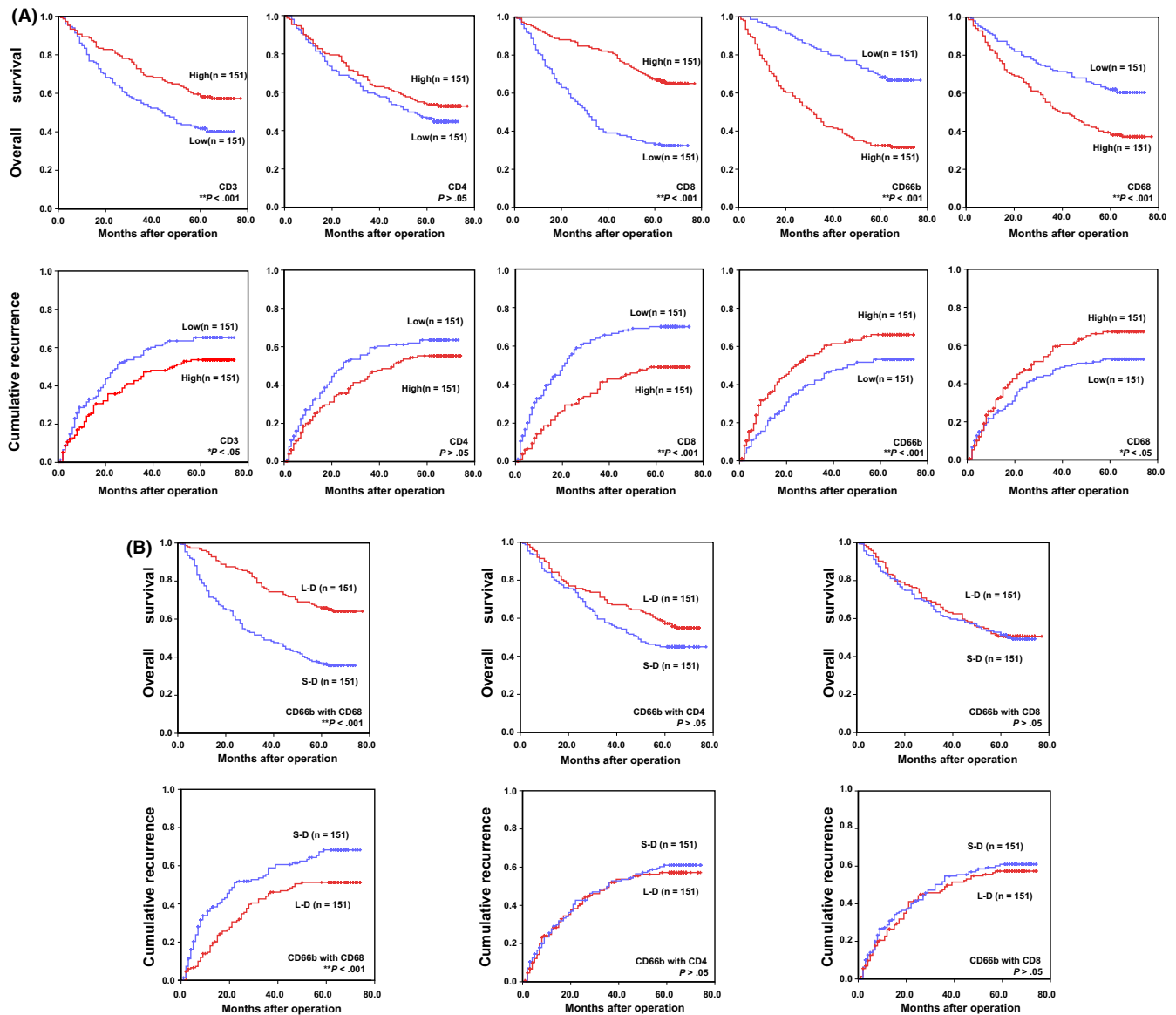


FIGURE 4 Correlation of different immune cells with clinical outcomes in 302 patients with primary HCC. A, Kaplan-Meier survival analysis showing how intratumoral CD3⁺, CD4⁺, CD8⁺, CD66b⁺ and CD68⁺ cells were associated with OS rates and cumulative recurrence rates after surgery. B, Kaplan-Meier survival analysis showing how the distance between 2 different immune cell subpopulations were associated with OS rates and cumulative recurrence rates after surgery. L-D (longer distance); S-D (shorter distance)

after surgical resection of HCC (Figure 4). Higher infiltrations of CD3⁺ T cells and CD8⁺ T cells were associated with better OS and lower cumulative recurrence rates ($**P < .001$ and $*P < .05$, $**P < .001$ for both, respectively; Figure 4A). Conversely, the presence of neutrophils and macrophages within HCC tumors was negatively correlated with OS and the cumulative recurrence rates ($**P < .001$ for both, $**P < .001$ and $*P < .05$, respectively; Figure 4A). However, the presence of CD4⁺ T cells within tumor was not associated with OS and cumulative recurrence rates ($P > .05$ for both, Figure 4A). The association of different immune cells in non-tumor liver tissues with patient prognosis shown in Figure S3.

We calculated the average distance between 2 different immune cell subpopulations, and values of r ranging from 0 to 30 μm .

The mean distances between neutrophils and macrophages, neutrophils and CD4⁺ T cells, and neutrophils and CD8⁺ T cells were 18.08, 20.28, and 19.59 μm , respectively. Furthermore, a shorter distance (S-D) between neutrophils and macrophages was associated with worse OS and higher cumulative recurrence rates ($**P < .001$ for both; Figure 4B). However, the distance between neutrophils and CD4⁺ T cells and neutrophils and CD8⁺ T cells was not correlated with OS or cumulative recurrence rates ($P > .05$ for both; Figure 4B).

Univariate and multivariate Cox proportional hazard models revealed that tumor size, microvascular invasion, and the presence of CD8⁺, CD66b⁺ and CD68⁺ cells in tumor tissues were independent prognostic factors for both OS and the time to recurrence (Table 2).

TABLE 2 Univariate and multivariate analyses of prognostic factors in HCC (n = 302)

Variable	TTR		OS	
	HR (95% CI)	P	HR (95% CI)	P
Univariate analysis				
Age, y (≤ 50 vs > 50)	0.918 (0.675-1.248)	.584	0.754 (0.547-1.040)	.086
Sex (female vs male)	1.767 (1.082-2.885)	.023	1.640 (0.977-2.755)	.061
HBsAg (negative vs positive)	1.118 (0.700-1.786)	.640	1.064 (0.683-1.658)	.783
AFP, ng/ml (≤ 20 vs > 20)	1.128 (0.807-1.576)	.482	1.587 (1.091-2.309)	.016
GGT, U/L (≤ 54 vs > 54)	1.304 (0.950-1.789)	.101	1.647 (1.174-2.313)	.004
Liver cirrhosis (no vs yes)	1.230 (0.723-2.093)	.444	1.305 (0.739-2.305)	.359
Tumor size, cm (≤ 5 vs > 5)	1.650 (1.208-2.254)	.002	2.139 (1.530-2.990)	.000
Tumor number (single vs multiple)	1.388 (0.922-2.089)	.116	1.605 (1.080-2.384)	.019
Microvascular invasion (no vs yes)	1.962 (1.438-2.676)	.000	2.488 (1.795-3.449)	.000
Tumor encapsulation (complete vs none)	1.718 (1.260-2.343)	.001	1.747 (1.262-2.417)	.001
Tumor differentiation (I + II vs III +IV)	1.198 (0.830-1.729)	.335	1.490 (1.034-2.145)	.032
TNM stage (I vs II III)	1.195 (0.879-1.624)	.256	1.482 (1.075-2.042)	.016
CD3 (low vs high)	0.713 (0.519-0.981)	.038	0.672 (0.489-0.925)	.015
CD4 (low vs high)	0.782 (0.569-1.073)	.128	0.800 (0.583-1.098)	.168
CD8 (low vs high)	0.370 (0.265-0.518)	.000	0.348 (0.249-0.488)	.000
CD66b (low vs high)	2.784 (1.981-3.914)	.012	3.137 (2.230-4.413)	.000
CD68 (low vs high)	1.764 (1.276-2.440)	.001	1.798 (1.301-2.484)	.000
Multivariate analysis				
Sex (female vs male)	2.171 (1.255-3.757)	.006	NA	NA
AFP, ng/ml (≤ 20 vs > 20)	NA	NA	1.328 (0.895-1.969)	.158
GGT, U/L (≤ 54 vs > 54)	NA	NA	1.458 (1.024-2.077)	.037
Tumor size, cm (≤ 5 vs > 5)	1.783 (1.247-2.549)	.002	1.820 (1.280-2.587)	.001
Tumor number (single vs multiple)	NA	NA	1.033 (0.675-1.579)	.883
Microvascular invasion (no vs yes)	1.480 (1.048-2.090)	.026	1.680 (1.187-2.379)	.003
Tumor encapsulation (complete vs none)	1.302 (0.982-1.828)	.127	1.111 (0.786-1.570)	.550
Tumor differentiation (I + II vs III +IV)	NA	NA	1.228 (0.882-1.711)	.224
TNM stage (I vs II III)	NA	NA	1.143 (0.867-1.506)	.345
CD3 (low vs high)	1.706 (0.493-1.009)	.056	0.673 (0.471-0.963)	.030
CD8 (low vs high)	0.297 (0.208-0.425)	.000	0.272 (0.189-0.390)	.000
CD66b (low vs high)	3.138 (2.182-4.514)	.000	3.326 (2.306-4.798)	.000
CD68 (low vs high)	2.039 (1.422-2.923)	.000	2.391 (1.665-3.435)	.000

Note: Cox proportional hazards regression model. AFP, alpha-fetoprotein; CI, confidential interval; GGT, gamma glutamyl transferase; HR, hazard ratio; NA, not adopted.

4 | DISCUSSION

The most common underlying cause of HCC is chronic infection with HBV or hepatitis C virus.¹⁶ The efficacy of immunology therapy in the treatment of patients with HCC remains unsatisfactory. One reason is that our understanding of the complex mechanisms by which HCC cells escape the body's immune response remains incomplete. Cancer progression is regulated by interactions between cancer cells and the surrounding microenvironment,¹⁷ and the immune system plays dual roles in malignancy development and progression.¹⁸ Some immune cells inhibit tumor growth, whereas others enhance malignancy

progression.¹⁹ To characterize the spatial distribution of immune cells, we performed multiplex IHC using tissue microarrays from 302 patients with primary HCC. Our results showed that the spatial distribution of immune cells is heterogeneous in the HCC TME.

The HCC tumor tissues contained fewer CD3⁺ T cells than the non-tumor tissues, a finding consistent with previous studies.^{20,21} Among T lymphocytes, CD8⁺ T lymphocytes were the predominant T-cell population. CXCR3-mediated CD8⁺ T cell trafficking into tumor tissues was associated with favorable outcomes in patients with cancers such as melanoma and ovarian cancer.²² In the present study, HCC patients with higher rates of CD8 expression

on tumor-infiltrating T cells had better outcomes after surgery. In addition, the percentage of CD4⁺ T cells within the CD3⁺ T-cell population was much higher in HCC tumors than in normal liver tissues. Importantly, CD4⁺ T cells play a critical role in antitumor immune function. Conventional effector CD4⁺ T cells enhance the ability of the immune system to eliminate tumor cells by stimulating pro-inflammatory programs and licensing dendritic cells.²³

Neutrophils are the first responders in the host immune defense against infection.²⁴ In the progression of primary tumors, chronic inflammation is a common aspect. The role of neutrophils in tumor biology has remained controversial, however.²⁵ Previous studies have shown that tumor patients with low numbers of tumor-infiltrating neutrophils have a better OS than those with a high number of tumor-infiltrating neutrophils.^{26,27} Consistent with those results, we discovered that increased numbers of neutrophils were associated with poor outcomes in HCC patients.

Macrophages are a large component of the infiltrating leukocyte compartment in the TME. Tumor-associated macrophages also exert immunosuppressive functions.²⁸ Kuang and colleagues reported that macrophages suppressed the response of T cells through PD-L1 in HCC.²⁹ We also discovered that patients with a low number of macrophages had a better prognosis.

In our previously study, we found tumor-associated neutrophils recruited macrophages to promote tumor progression by secreting CCL2.^{9,30} The results of G(r) and K(r) functions supported the observation that neutrophils and macrophages aggregated closer together. Furthermore, we discovered that a longer distance between neutrophils and macrophages was associated with a better prognosis. In TME, CD8⁺ T cells and neutrophils play different roles in predicting patient prognosis. Some groups have reported that neutrophils play a critical role in recruiting of CD8⁺ T cells and frequently colocalize with CD8⁺ T cells in colorectal cancer.³¹⁻³³ In our study, G(r) and K(r) functions indicated that CD8⁺ T cells and neutrophils tended to aggregate closer together. However, the distance between neutrophils and CD8⁺ T cells was not correlated with patient prognosis after surgery. We suggest that a mechanism of interaction exists between a certain subgroup of CD8⁺ T cells and neutrophils, but this does not influence neutrophils and CD8⁺ T cells as independent prognostic predictors. The cross-talk between neutrophils and CD8⁺ T cells has not been investigated. Therefore, our future studies could explore the mechanism of interaction between CD8⁺ T cells and neutrophils.

Multiplex IHC allows the evaluation of different cell subsets on a single slide. Two tumor cores and 2 cores of normal liver tissues were available for each patient. In addition, false-positive results are a common problem in single-marker IHC studies. Our study used co-localization to improve the accuracy of the experimental results. The use of multiple markers allows the elucidation of different immune cell subsets in a single tissue section. This study is the first to use G(r) and K(r) functions to simultaneously characterize the spatial relationships among different immune cell subpopulations in HCC tumors and analyze the association of the distance between 2 different immune cells with patients' prognosis using Euclidean distance.

Our study illustrated the spatial distribution of several critical immune cell types. In the past decades, all researchers have reached a consensus that tumor cells grow in a complex tissue microenvironment. Sia and colleagues presented gene profiles of HCC TME using a non-negative matrix factorization algorithm and discovered a novel immune specific class which might be an ideal candidate for an immunotherapy target, such as the PD-L1 inhibitor.³⁴ We did not take a deeper exploration to represent a comprehensive characterization of HCC TME. So, we need to validate our research in a larger patient cohort and focus on the mechanism that may provide a theoretical basis for clinical treatment.

In summary, interactions between tumor cells and immune cells and the relationships between different immune cell subpopulations are essential properties of the TME. Our results provide a picture of the TME immune cell composition. The mechanisms of the pathophysiological interactions in the TME need to be explored further.

ACKNOWLEDGMENTS

This study was jointly supported by Major Special Projects of the Ministry of Science and Technology (2018ZX10302207), National Natural Science Foundation of China (91942313, 81472672), Shanghai International Science and Technology Collaboration Program (18410721900), and Fundamental Medical Project of Minhang Hospital of the Fudan University Project Foundation (Grant N. 2020MHJC06).

DISCLOSURE

Authors declare no conflicts of interest for this article.

ORCID

Peng-Cheng Wang  <https://orcid.org/0000-0001-7333-355X>

Shao-Lai Zhou  <https://orcid.org/0000-0002-8526-5221>

REFERENCES

1. Siegel RL, Miller KD, Jemal A. Cancer statistics, 2018. *CA Cancer J Clin.* 2018;68:7-30.
2. Llovet JM, Sala M, Castells L, et al. Randomized controlled trial of interferon treatment for advanced hepatocellular carcinoma. *Hepatology.* 2000;31:54-58.
3. Zacharakis N, Chinnasamy H, Black M, et al. Immune recognition of somatic mutations leading to complete durable regression in metastatic breast cancer. *Nat Med.* 2018;24:724-730.
4. Liu P, Zhao L, Pol J, et al. Crizotinib-induced immunogenic cell death in non-small cell lung cancer. *Nat Commun.* 2019;10:1486.
5. Ringelhan M, Pfister D, O'Connor T, Pikarsky E, Heikenwalder M. The immunology of hepatocellular carcinoma. *Nat Immunol.* 2018;19:222-232.
6. Quail DF, Joyce JA. Microenvironmental regulation of tumor progression and metastasis. *Nat Med.* 2013;19:1423-1437.
7. Maman S, Witz IP. A history of exploring cancer in context. *Nat Rev Cancer.* 2018;18:359-376.
8. Garris CS, Arlauckas SP, Kohler RH, et al. Successful anti-PD-1 cancer immunotherapy requires T cell-dendritic cell crosstalk involving the cytokines IFN-gamma and IL-12. *Immunity.* 2018;49:1148-1161 e1147.
9. Zhou S-L, Zhou Z-J, Hu Z-Q, et al. Tumor-associated neutrophils recruit macrophages and T-regulatory cells to promote

- progression of hepatocellular carcinoma and resistance to Sorafenib. *Gastroenterology*. 2016;150(7):1646-1658 e17.
10. Prestipino A, Zeiser R. Clinical implications of tumor-intrinsic mechanisms regulating PD-L1. *Sci Transl Med*. 2019;11.
 11. Zhou S-L, Dai Z, Zhou Z-J, et al. Overexpression of CXCL5 mediates neutrophil infiltration and indicates poor prognosis for hepatocellular carcinoma. *Hepatology*. 2012;56:2242-2254.
 12. Wittekind C. Pitfalls in the classification of liver tumors. *Pathologie*. 2006;27:289-293.
 13. Zhou ZJ, Dai Z, Zhou SL, et al. HNRNPAB induces epithelial-mesenchymal transition and promotes metastasis of hepatocellular carcinoma by transcriptionally activating SNAIL. *Can Res*. 2014;74:2750-2762.
 14. Carstens JL, Correa de Sampaio P, Yang D, et al. Spatial computation of intratumoral T cells correlates with survival of patients with pancreatic cancer. *Nat Commun*. 2017;8:15095.
 15. Angelova M, Mlecnik B, Vasaturo A, et al. Evolution of metastases in space and time under immune selection. *Cell*. 2018;175:751-765 e16.
 16. de Martel C, Maucourt-Boulch D, Plummer M, Franceschi S. World-wide relative contribution of hepatitis B and C viruses in hepatocellular carcinoma. *Hepatology*. 2015;62:1190-1200.
 17. Hanahan D, Coussens LM. Accessories to the crime: functions of cells recruited to the tumor microenvironment. *Cancer Cell*. 2012;21:309-322.
 18. Zamarron BF, Chen W. Dual roles of immune cells and their factors in cancer development and progression. *Int J Biol Sci*. 2011;7:651-658.
 19. Galon J, Bruni D. Tumor immunology and tumor evolution: intertwined histories. *Immunity*. 2020;52:55-81.
 20. Gao Q, Zhou J, Wang X-Y, et al. Infiltrating memory/senescent T cell ratio predicts extrahepatic metastasis of hepatocellular carcinoma. *Ann Surg Oncol*. 2012;19:455-466.
 21. Fu J, Xu D, Liu Z, et al. Increased regulatory T cells correlate with CD8 T-cell impairment and poor survival in hepatocellular carcinoma patients. *Gastroenterology*. 2007;132:2328-2339.
 22. Mikucki ME, Fisher DT, Matsuzaki J, et al. Non-redundant requirement for CXCR3 signalling during tumoricidal T-cell trafficking across tumour vascular checkpoints. *Nat Commun*. 2015;6:7458.
 23. Eickhoff S, Brewitz A, Gerner M, et al. Robust anti-viral immunity requires multiple distinct T cell-dendritic cell interactions. *Cell*. 2015;162:1322-1337.
 24. Singel KL, Segal BH. Neutrophils in the tumor microenvironment: trying to heal the wound that cannot heal. *Immunol Rev*. 2016;273:329-343.
 25. Powell DR, Huttenlocher A. Neutrophils in the tumor microenvironment. *Trends Immunol*. 2016;37:41-52.
 26. Zhou S-L, Yin D, Hu Z-Q, et al. A positive feedback loop between cancer stem-like cells and tumor-associated neutrophils controls hepatocellular carcinoma progression. *Hepatology*. 2019;70(4):1214-1230.
 27. Jensen HK, Donskov F, Marcussen N, Nordmark M, Lundbeck F, von der Maase H. Presence of intratumoral neutrophils is an independent prognostic factor in localized renal cell carcinoma. *J Clin Oncol*. 2009;27:4709-4717.
 28. Pappas AG, Magkouta S, Pateras IS, et al. Versican modulates tumor-associated macrophage properties to stimulate mesothelioma growth. *Oncoimmunology*. 2019;8:e1537427.
 29. Kuang D-M, Zhao Q, Peng C, et al. Activated monocytes in peritumoral stroma of hepatocellular carcinoma foster immune privilege and disease progression through PD-L1. *J Exp Med*. 2009;206:1327-1337.
 30. Zhou Z, Wang P, Sun R, et al. Tumor-associated neutrophils and macrophages interaction contributes to intrahepatic cholangiocarcinoma progression by activating STAT3. *J Immuno Therapy Cancer*. 2021;9(3):e001946.
 31. de Oca RM, Buendia AJ, Del Rio L, Sanchez J, Salinas J, Navarro JA. Polymorphonuclear neutrophils are necessary for the recruitment of CD8(+) T cells in the liver in a pregnant mouse model of *Chlamydomydia abortus* (*Chlamydia psittaci* serotype 1) infection. *Infect Immun*. 2000;68:1746-1751.
 32. Lim K, Hyun YM, Lambert-Emo K, et al. Neutrophil trails guide influenza-specific CD8(+) T cells in the airways. *Science*. 2015;349:aaa4352.
 33. Governa V, Trella E, Mele V, et al. The interplay between neutrophils and CD8(+) T cells improves survival in human colorectal cancer. *Clin Cancer Res*. 2017;23:3847-3858.
 34. Sia D, Jiao Y, Martinez-Quetglas I, et al. Identification of an immune-specific class of hepatocellular carcinoma, based on molecular features. *Gastroenterology*. 2017;153:812-826.

SUPPORTING INFORMATION

Additional supporting information may be found in the online version of the article at the publisher's website.

How to cite this article: Wang P-C, Hu Z-Q, Zhou S-L, et al. The spatial distribution of immune cell subpopulations in hepatocellular carcinoma. *Cancer Sci*. 2022;113:423-431. doi:[10.1111/cas.15202](https://doi.org/10.1111/cas.15202)